J|A|C|S
ARTICLES
Published on Web 11/01/2002

An NMR Study of the Solution Dynamics of Deltorphin-I

Marie-Thérèse Chenon[†] and Lawrence G. Werbelow*[,‡]

Contribution from the LADIR−CNRS, 2 rue Henry Dunant, 94320 Thiais, France and Arrhenius Laboratory, Stockholm University, 10691 Stockholm, Sweden

Received June 3, 2002. Revised Manuscript Received July 29, 2002

Abstract: Nuclear spin relaxation rates associated with cross-correlated, dipole−dipole interactions are enlisted to help characterize the solution state dynamics of a small heptapeptide, deltorphin-I. A simple two-site jump model can be used to interpret the data obtained on two specific ^{13}C labeled residues, D-alanine and glycine. The influence of temperature and solvent upon the observed dynamics is investigated. Similarly, relaxation rates associated with dipole-shielding anisotropy interferences are used to examine the magnitude and orientation of various chemical shielding tensors within the D-alanine and glycine residues.

Introduction

Contemporary biomolecular applications of nuclear magnetic resonance (NMR) often rely upon the determination of nuclear spin relaxation parameters that embody both structural and dynamic information sampled at the submicroscopic level.[1−7] Ultimately, the credibility of these studies depends on the soundness of the methodology used for isolating and identifying this complementary information that is entangled in a complex manner. Tradeoffs between exacting theoretical descriptions and more tractable approximations permitted by limited data sets must be considered. Often, data sets include the orientational relaxation behavior of only one vector per residue (mainly the NH bond) using variations on the popular Lipari−Szabo model[8] or the spectral density mapping approach introduced explicitly by Peng and Wagner.[9] The overall tumbling motions as well as the local motions are usually considered as isotropic although sometimes the anisotropies are taken into account.[10]

In contrast, exploitation of relaxation-induced polarization or coherence transfer[11] that utilizes the correlated relaxation properties of two or more vectors per residue provides a robust alternative approach for the study of biomolecular dynamics and recently, there has been keen interest in exploiting this resource.[6,7,12−18] The use of motional restriction maps of auto- and cross-correlation order parameters introduced by Daragan and Mayo[19] illustrates this approach nicely. Some researchers have gone further. For example, Zuiderweg and co-workers[20] have characterized qualitatively the anisotropic local dynamics of several peptide planes of a 20 kDa protein by investigating the temporal cross-correlation (interference) between competitive relaxation pathways. Here, the unique features associated with these cross-correlation spectral densities permitted the clear discrimination between different dynamic models. These authors emphasized that it is important to measure relaxation parameters of several vectors in a motional unit to describe the dynamic properties properly. Furthermore, these authors explicitly reject the notion that local and semi-local peptide-plane dynamics are isotropic.

In the presented work, the specific role of dipole−dipole (D × D) and dipole-shielding anisotropy (D × SA) cross-correlated spectral densities and their potential for revealing the local dynamics of small biomolecules is investigated. A heptapeptide that had been studied by simulated annealing on the basis of

* Address correspondence to this author. Permanent address: Chemistry, NMIMT, Socorro, NM 87801. E-mail: werbelow@nmt.edu.
[†] LADIR−CNRS.
[‡] Stockholm University.

(1) Mayo, K. H.; Daragan, V. A. *Protein Dynamics NMR Relaxation;* Imperial College Press: London, 2002.
(2) Luginbuhl, P.; Wüthrich, K. *Prog. Nucl. Magn. Reson. Spectrosc.* **2002**, *40*, 199−247.
(3) Korzhnev, D. M.; Billeter, M.; Arseniev, A. S.; Orekhov, V. Y. *Prog. Nucl. Magn. Reson. Spectrosc.* **2001**, *38*, 197−266.
(4) Palmer, A. G. *Annu. Rev. Biophys. Biomol. Struct.* **2001**, *30*, 129−155.
(5) Dayie, K. T.; Wagner, G.; Lefèvre, J.-F. *Annu. Rev. Phys. Chem.* **1996**, *47*, 243−282.
(6) Fischer, M. W. F.; Majumdar, A.; Zuiderweg, E. R. P. *Prog. Nucl. Magn. Reson. Spectrosc.* **1998**, *33*, 207−272.
(7) Daragan, V. A.; Mayo, K. H. *Prog. Nucl. Magn. Reson. Spectrosc.* **1997**, *32*, 63−105.
(8) Lipari, G.; Szabo, A. *J. Am. Chem. Soc.* **1982**, *104*, 4546−4558.
(9) Peng, J. W.; Wagner, G. *J. Magn. Reson.* **1992**, *98*, 308−332. Peng, J. W.; Wagner, G. *Methods Enzymol.* **1993**, *239*, 563−596.
(10) Daragan, V. A.; Mayo, K. H. *J. Phys. Chem. B* **1999**, *103*, 6829−6834. Deschamps, M. *J. Phys. Chem. A* **2002**, *106*, 2438−2445. Deschamps, M.; Bodenhausen, G. *ChemPhysChem* **2001**, *2*, 539−543.
(11) Werbelow, L. G. *Nuclear Magnetic Resonance Probes of Molecular Dynamics*; Tycko, R. Ed.; Plenum: New York, 1994; pp 223−263.
(12) Brutscher, B. *Concepts Magn. Reson.* **2000**, *12*, 207−229.
(13) Pellecchia, M.; Pang, Y.; Wang, L.; Kurochkin, A. V.; Kumar, A.; Zuiderweg, E. R. P. *J. Am. Chem. Soc.* **1999**, *121*, 9165−9170. Pang, Y.; Wang, L.; Pellecchia, M.; Kurochkin, A. V.; Zuiderweg, E. R. P. *J. Biomol. NMR* **1999**, *14*, 297−306.
(14) Bremi, T.; Ernst, M.; Ernst, R. R. *J. Phys. Chem.* **1994**, *98*, 9322−9334. Ernst, M.; Ernst, R. R. *J. Magn. Reson. A* **1994**, *110*, 202−213. Bremi, T.; Brüschweiler, R.; Ernst, R. R. *J. Am. Chem. Soc.* **1997**, *119*, 4272−4284.
(15) Lienin, S. F.; Bremi, T.; Brutscher, B.; Brüschweiler, R.; Ernst, R. R. *J. Am. Chem. Soc.* **1998**, *120*, 9870−9879. Scheurer, C.; Skrynnikov, N. R.; Lienin, S. F.; Straus, S. K.; Brüschweiler, R.; Ernst, R. R. *J. Am. Chem. Soc.* **1999**, *121*, 4242−4251.
(16) Daragan, V. A.; Mayo, K. H. *Biochemistry* **1993**, *32*, 11488−11499.
(17) Daragan, V. A.; Mayo, K. H. *J. Magn. Reson.* **1998**, *130*, 329−334.
(18) Felli, I. C.; Desvaux, H.; Bodenhausen, G. *J. Biomol. NMR* **1998**, *12*, 509−521. Yang, D.; Mok, Y.-K.; Muhandiram, D. R.; Forman-Kay, J. D.; Kay, L. E. *J. Am. Chem. Soc.* **1999**, *121*, 3555−3556.
(19) Daragan, V. A.; Mayo, K. H. *J. Magn. Reson. B* **1995**, *107*, 274−278.
(20) Fischer, M. W. F.; Zeng, L.; Pang, Y.; Hu, W.; Majumdar, A.; Zuiderweg, E. R. P. *J. Am. Chem. Soc.* **1997**, *119*, 12629−12642.

10.1021/ja020772q CCC: $22.00

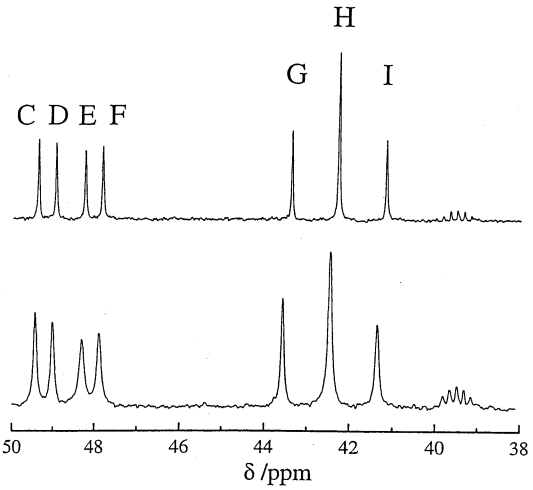

Figure 1. Proton-coupled $^{13}C_\alpha$ spectra of the D-alanine (resonances C, D, E, and F) and glycine (resonances G, H, and I) residues of Deltophin-I obtained for a 20 mM solution in DMSO-d_6/D_2O 80/20 v/v. The upper spectrum was obtained at 314 K and the lower spectrum at 265 K. DMSO-d_6 was used as an internal reference at 39.5 ppm at both temperatures.

NMR restraints,[21] deltorphin-I, Tyr(D-Ala)PheAsp(Val)$_2$GlyNH$_2$, was chosen for study. In particular, the two residues, D-alanine and glycine, each having very different mobility, were examined. Of course, exacting NMR relaxation measurements are used for purposes other than investigation of molecular dynamics on the nanosecond time scale and it was anticipated that details about certain shielding tensors and possible indications of the existence of various solution-state conformers obtained by modeling calculations[21] would be forthcoming from this study.

Experimental Section

Synthesis and Sample Preparation. To increase the signal/noise ratio, the C_α and carbonyl (C′) carbons of D-alanine were enriched in ^{13}C. Furthermore, to minimize extraneous dipole−dipole interactions, the methyl group of D-alanine was deuterated. This D-residue was synthesized using [1,2-$^{13}C_2$]-glycine and deuterated iodomethane. Both compounds were purchased from Isotec. D-alanine was obtained by alkylation of the sultam-glycinate derivative as described in the literature.[22] Likewise, ^{13}C enriched (at C_α) glycine was purchased from the same vendor. The nitrogen atom of both these compounds was protected by a Boc group[23] before incorporation into the peptide.

Two samples were studied: (i) a 13 mM solution in DMSO-d_6/D_2O 98/2 v/v (solution I), at 298 and 310 K (this facilitated the comparison of our NMR data with supplemental data already obtained at LADIR[21]) and (ii) a 20 mM solution in DMSO-d_6/D_2O 80/20 v/v (solution II), at 265 K (to compare with literature data[21]) and 314 K. At 314 K, solution II has the same (macroscopic) viscosity (2.12 cp) as solution I at 298 K and thus, the medium's influence on the dynamics could be addressed. Because of the proximity between the solvent and C_α(Gly) resonances as shown in Figure 1, the DMSO-d_6 purchased (Isotec) was ^{13}C depleted. Despite the treatment of the ^{12}C-DMSO-d_6 with D_2O to eliminate H_2O, it proved necessary to add a small amount of D_2O to solution I to exchange (remove) the nitrogen proton.

To obtain spectra with good signal/noise ratios in a reasonable amount of time, relatively concentrated solutions were used in this study. As revealed by a study of proton chemical shift versus concentration,[24] these concentrations do not induce auto-association of deltorphin-I at ambient temperature. Conversely, such auto-association appears to occur at 265 K.

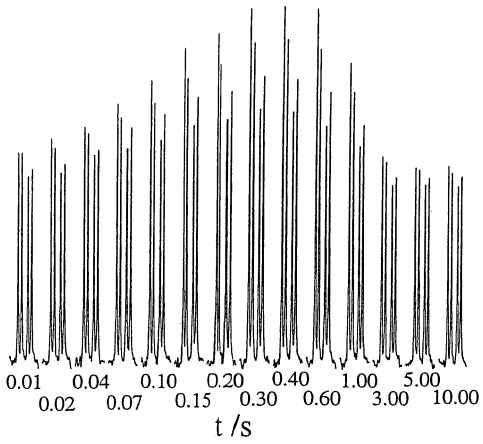

Figure 2. Evolution of the normalized $^{13}C_\alpha$ magnetization of D-alanine for different times between perturbation (H_α inversion) and observation. This response is shown for Solution I at 310 K.

NMR Spectroscopy and Data Processing. Spectra were obtained on a Varian vxr-500 spectrometer. IBURP and EBURP pulses[25] were used for inversion and observation of the carbon magnetization, respectively. These carefully calibrated semiselective pulses were used to prevent the erasure of the characteristic signature of DD × SA interferences.[26] Pulse effectiveness (>90%) was taken into account in data analysis.

The response characteristics of the carbon (C′ or C_α) magnetizations were observed after various perturbations of either the carbon (C′ or C_α) or the proton (H_α) magnetization (i.e., hard pulse, soft pulse, or *J*-pulse preparations). For example, in Figure 2, the response of the D-alanine C_α magnetization after H_α inversion (the transient Overhauser experiment) is shown. This figure clearly demonstrates the creation and dissipation of multispin order as relaxation processes restore Boltzmann order.

Spectra were analyzed with the 1D_ANALYSIS program.[27] For the C′ multiplet, in addition to the intraresidue ^2J coupling (4.5 Hz) with H_α, a ^3J coupling (2.9 Hz) with H_α(Phe) (neighboring residue) was considered. For solution I, the isotopic effect due to the NH residues yields C_α patterns at ≈0.07 ppm (higher frequency) from those of the major ND species. This isotopic effect was considered in the analysis of the spectra despite the small amount of the NH species (less than 10%). For each experiment, the intensity of each line was normalized, independently, by comparison with the thermal equilibrium value. Only the carbon data obtained after inversion of either one carbon or the H_α protons are considered in this paper. For sake of discussion, the individual multiplet components of the C_α carbons are labeled progressively from high frequency to low frequency (lines C to I respectively; see Figure 1). The two, complex, low-field components (see above) associated with C′ are not utilized in this analysis.

Theory

The basic theory necessary to analyze fundamental relaxation features in scalar coupled spin systems is well understood.[28−30] For the glycine moiety, the observed spin system approximates

(21) Naim, M.; Nicolas, P.; Benajiba, A.; Baron, D. *J. Peptide Res*. **1998**, *52*, 443−457.
(22) Oppolzer, W.; Moretti, R.; Thomi, S. *Tetrahedron Lett.* **1989**, *30*, 6009−6010. Josien, H.; Martin, A.; Chassaing, G. *Tetrahedron Lett.* **1991**, *32*, 6547−6550.
(23) *Organic Syntheses*; Wiley: New York, 1990; Collect. Vol. VII, p 70.
(24) Chenon, M.-T. Unpublished data.
(25) Geen, H.; Freeman, R. *J. Magn. Reson.* **1991**, *93*, 93−141.
(26) Nery, H.; Canet, D. *J. Magn. Reson*. **1981**, *42*, 370−380.
(27) Chenon, M.-T.; Dunkel, R.; Grant, D. M.; Werbelow, L. G. *J. Phys. Chem. A* **1999**, *103*, 1447−1456.
(28) Kumar, A.; Grace, C. R.; Madhu, P. K. *Prog. Nucl. Magn. Reson. Spectrosc.* **2000**, *37*, 191−319.
(29) Werbelow, L. G. *Encyclopedia of Nuclear Magnetic Resonance*; Grant, D. M., Harris, R. K., Eds.; Wiley: London, 1996; pp 4072−4078.
(30) Werbelow, L. G.; Thevand, A.; Pouzard, G. *J. Chim. Phys. (Paris)* **1979**, *76*, 722−730.

an AX_2 ($^{13}C_\alpha H_2$) grouping. For the alanine moiety, use is made of the embedded AMX ($^{13}C'^{13}C_\alpha H_\alpha$) spin system. In either instance, the appropriate equations can be written in the compact form $-(d/dt)\ \boldsymbol{\nu}_i = \boldsymbol{\Gamma}_{ij}\boldsymbol{\nu}_j$ where the magnetization or coherence modes, $\boldsymbol{\nu}_i$, are identified with various observables such as two spin longitudinal order, $<2I_zS_z(t)>$ or doubly antiphase single quantum coherence, $<4I_+S_zS_z'(t)>$. Generally, the pure relaxation rates, $\boldsymbol{\Gamma}_{ii}$, are written as simple linear combinations of various auto-correlated spectral density functions whereas the polarization/coherence transfer rates, $\boldsymbol{\Gamma}_{ij}$, are identified with specific cross-correlated spectral density functions.

The transfer rates utilized in this study include the following:[29] for glycine,

$$S_z + S_z' \Rightarrow 2\sigma[C_\alpha H_\alpha] \Rightarrow I_z;\ S_z + S_z' \Rightarrow 4K^{D\times D}[C_\alpha H_\alpha{\cdot}H_\alpha H_\alpha'](\omega_H) \Rightarrow 4\, I_z S_z\, S_z';$$
$$\text{and } I_z \Rightarrow 2K^{D\times D}[C_\alpha H_\alpha{\cdot}C_\alpha H_\alpha'](\omega_C) \Rightarrow 4\, I_z S_z\, S_z';$$
$$\text{and for D-alanine, } S_z \Rightarrow \sigma[C_\alpha H_\alpha] \Rightarrow I_z;\ S_z \Rightarrow \sigma[C'H_\alpha] \Rightarrow I_z';\ I_z \Rightarrow \sigma[C'C_\alpha] \Rightarrow I_z';\ S_z \Rightarrow 2K^{D\times D}[C_\alpha H_\alpha{\cdot}H_\alpha C'](\omega_H) \Rightarrow 4\, I_z I_z' S_z;\ I_z \Rightarrow 2K^{D\times D}[H_\alpha C_\alpha{\cdot}C_\alpha C'](\omega_C) \Rightarrow 4\, I_z I_z' S_z, \text{ and } I_z' \Rightarrow 2K^{D\times D}[H_\alpha C'{\cdot}C'C_\alpha](\omega_C) \Rightarrow 4\, I_z I_z' S_z.$$

Angular momenta S and I associate with ^1H and ^{13}C spin, respectively. The cross-relaxation rates are defined as

$$\sigma[ij] = (-1/3)\ J^D[ij](\omega_i - \omega_j) + 2\ J^D[ij]\,(\omega_i + \omega_j) \quad (1)$$

where

$$J^D[ij](\omega) = (\xi_{ij})^2\, \mathrm{Re}\int_0^\infty <Y_2^{\,0}(\Omega_{ij}(t))\ Y_2^{\,0}(\Omega_{ij}(0))> \exp(-i\omega t)\, dt \quad (2)$$

The dipole−dipole interaction constant between spins i and j, $\xi_{ij} = (6\pi/5)^{1/2}(\mu_o/4\pi)\gamma_i\gamma_j\hbar<r_{ij}^{-3}>$, incorporates appropriately weighted internuclear distances and gyromagnetic ratios. The angular arguments of the normalized spherical harmonics position the internuclear axis in the laboratory frame and thus, incessant molecular motion renders these time dependent. The dipole−dipole cross-correlated rates are defined similarly:

$$K^{D\times D}[ij{\cdot}jk](\omega) = \xi_{ij}\xi_{jk}\mathrm{Re}\int_0^\infty <Y_2^{\,0}(\Omega_{ij}(t))\ Y_2^{\,0}(\Omega_{jk}(0))> \exp(-i\omega t)\, dt \quad (3)$$

In addition, numerous transfer rates involving both carbon and proton shielding anisotropies are determined in this study. However, for nonaxially symmetric interactions such as shielding anisotropy, it proves impossible to discriminate between interaction constants, geometrical factors, and dynamic parameters and the functional simplicity of eqs 2 and 3 is lost. Understandably, these rates are not written easily in a friendly form. Later, this will be illustrated by example.

Although the framework describing the evolution of various observable magnetizations and coherences is exacting and relatively simple, the molecular interpretation of the spectral densities remains quite challenging.[31] Suffice to say that the interpretational method of overwhelming choice has been the model introduced explicitly by Lipari and Szabo[8] and implicitlyby others. This simplified model presumes that the appropriate orientational time-correlation function is biexponential. Although often unstated, this functional form further implies that the two components decay on different time scales with the faster decay effectively reducing the strength of interaction. There are certain scenarios where such a simple description may work reasonably well, but in most instances, this model is neither adequate nor applicable and more sophisticated modeling should be considered.

Results

Determination of the Spectral Densities. Numerous cross-correlated spectral densities can be identified uniquely from the initial response of various magnetization modes after carbon or proton inversion.[30] Thus, these spectral densities can be obtained either by numerical extrapolation or by fitting algorithms using complete data sets. It is our experience that the two approaches yield similar results. Zero frequency or adiabatic spectral densities were determined from differences between transverse relaxation rates (ΔR_2) which in turn were determined from the thermal equilibrium spectra using the 1D_ANALYSIS program.[27] Inhomogeneous broadenings were small compared with the natural line widths.

All of the experimentally deduced spectral densities utilized in subsequent analysis are summarized in Table 1. Also shown in this table are calculated values determined from the analysis described in subsequent sections of this manuscript.

Interpretation of the Spectral Densities. Even for relatively simple systems, modeling the various spectral densities is nontrivial. Meticulous studies by Ernst and co-workers[14−15] illustrate this nicely. After considering a large number of models (restricted rotational diffusion, unrestricted rotational diffusion, three-site jumps with equal populations, three site jumps with unequal populations, two site jumps, etc.), these workers concluded,[32] "It is not feasible to explore the dynamical properties to such an extent as it is possible to characterize a rigid geometry. The complexity of the motional quest is by order of magnitudes greater than a structure determination."

Of course, much of this complexity is obscured when the (auto-correlated) spectral density function relevant for NMR relaxation analyses is modeled mathematically as a normalized sum of Lorentzians:

$$J(\omega) \propto \mathrm{Re}\int_0^\infty \exp(-t/\tau_0)\{S_1^{\,2}\cdots S_n^{\,2} + (1 - S_n^{\,2})\exp(-t/\tau_n) + S_n^{\,2}(1 - S_{n-1}^{\,2})\exp(-t/\tau_{n-1}) + \ldots + S_n^{\,2}S_{n-1}^{\,2}\cdots S_2^{\,2}(1 - S_1^{\,2})\exp(-t/\tau_1)\}\exp(-i\omega t)\, dt \quad (4)$$

In this notation, $S_n^{\,2}S_{n-1}^{\,2}\cdots S_p^{\,2}(1 - S_{p-1}^{\,2})$ is simply the weight of the pth exponential associated with the time constant, τ_p. Each of the "order parameters," $S_p^{\,2}$, is intrinsically positive. (If $\tau_n = 0$ for all n except $n = 1$, the familiar Lipari−Szabo expression results and if $1/\tau_n = 0$ for all n other than $n = 0$, the bracketed term is unity.) Unfortunately, for the simplest physical model consisting of isotropic rotational diffusion ($1/\tau_0 = 6D$) with one

(31) See, for example: Prompers, J. J.; Brüschweiler, R. *J. Am. Chem. Soc.* **2002**, *124*, 4522−4534. Idiyatullin, D.; Daragan, V. A.; Mayo, K. H. *J. Magn. Reson.* **2001**, *152*, 132−148.

(32) Ernst, R. R.; Blackledge, M. J.; Bremi, T.; Brüschweiler, R.; Ernst, M.; Griesinger, C.; Madi, Z. L.; Peng, J. W.; Schmidt, J. M.; Xu, P. *NMR As a Structural Tool for Macromolecules*; Nageswara Rao, B. D., Kemple, M. D., Eds.; Plenum: New York, 1996; pp 15−34.

Table 1. Listing of Experimental and Modeled or Calculated Relaxation Rates and Polarization Transfer Rates Determined for (a) Solution I at 298 and 310 K and (b) Solution II at 265 and 314 K

	(a) Solution I at 298 and 310 K				(b) Solution II at 265 and 314 K			
	298 K		310 K		265 K		314 K	
spectral density (rad/s)	exptl	calcd	exptl	calcd	exptl	calcd	exptl	calcd
				Glycine				
$R_1[C_\alpha]$	3.92 ± 0.08	3.98[a]	3.45 ± 0.07	3.51[a]	4.58 ± 0.09	4.61[a]	3.78 ± 0.08	3.79[a]
$\sigma[C_\alpha H_\alpha]$	0.52 ± 0.02	0.50	0.521 ± 0.016	0.505	0.344 ± 0.016	0.344	0.512 ± 0.017	0.494
$K^{D\times D}[H_\alpha C_\alpha \cdot C_\alpha H_{\alpha'}](\omega_C)$	-0.13 ± 0.02	−0.11	-0.092 ± 0.015	−0.078	-0.447 ± 0.018	−0.444	-0.141 ± 0.017	−0.125
$K^{D\times D}[C_\alpha H_\alpha \cdot H_\alpha H_{\alpha'}](\omega_H)$	0.215 ± 0.011	0.224	0.218 ± 0.015	0.240	0.136 ± 0.009	0.129	0.224 ± 0.012	0.240
$K^{D\times SA}[C_\alpha H_\alpha \cdot H_\alpha](\omega_H)$	0.015 ± 0.001	0.016[b]	0.016 ± 0.001	0.016[b]	0.019 ± 0.004	0.011[b]	0.019 ± 0.004	0.016[b]
$K^{D\times SA}[H_\alpha C_\alpha \cdot C_\alpha](\omega_C)$	-0.08 ± 0.02	−0.069[c]	-0.054 ± 0.005	−0.055[c]	-0.099 ± 0.017	−0.103[c]	-0.064 ± 0.008	−0.063[c]
		−0.071[d]		−0.057[d]		−0.089[d]		−0.064[d]
$K^{D\times SA}[H_\alpha C_\alpha \cdot C_\alpha](0)$	-0.15 ± 0.05	−0.084[c]	-0.10 ± 0.04	−0.062[c]	-0.83 ± 0.09	−0.32[c]	-0.096 ± 0.014	−0.072[c]
		−0.089[d]		−0.066[d]		−0.29[d]		−0.074[d]
$J^{SA}[C_\alpha](\omega_C)$		0.010[d]		0.009[d]		0.014[d]		0.011[d]
ΔR_2[G−I]	-2.2 ± 0.3		-1.4 ± 0.3		-9.7 ± 0.8		-1.54 ± 0.08	
				D-Alanine				
$R_1[C_\alpha]$	3.48 ± 0.07	3.48[a]	3.51 ± 0.07	3.49[a]	1.88 ± 0.04	1.88[a]	3.51 ± 0.07	3.50[a]
$R_1[C']$	0.99 ± 0.02	0.79	0.95 ± 0.03	0.71	0.533 ± 0.011	0.499	0.95 ± 0.02	0.89
$\sigma[C_\alpha H_\alpha]$	0.45 ± 0.02	0.45	0.55 ± 0.02	0.55	0.154 ± 0.017	0.147	0.52 ± 0.02	0.52
$\sigma[H_\alpha C']$	0.010 ± 0.004	0.008	0.012 ± 0.02	0.012	0.007 ± 0.001	0.008	0.015 ± 0.004	0.015
$\sigma[C'C_\alpha]$	$<\|0.015\|$	−0.013	$<\|0.015\|$	−0.002	-0.098 ± 0.009	−0.096	$<\|0.015\|$	−0.010
$K^{D\times D}[C'C_\alpha \cdot C_\alpha H_\alpha](\omega_C)$	-0.076 ± 0.018	−0.081	-0.09 ± 0.02	−0.09	-0.027 ± 0.007	−0.031	-0.14 ± 0.03	−0.12
$K^{D\times D}[C'C_\alpha \cdot C_\alpha H_\alpha](0)$	-0.37 ± 0.14	−0.47	-0.21 ± 0.17	−0.41	-1.9 ± 0.5	−2.0	-0.17 ± 0.09	−0.46
$K^{D\times D}[C_\alpha H_\alpha \cdot H_\alpha C'](\omega_H)$	0.035 ± 0.006	0.038	0.039 ± 0.008	0.045	0.009 ± 0.004	0.010	0.032 ± 0.05	0.032
$K^{D\times D}[H_\alpha C' \cdot C'C_\alpha](\omega_C)$	<0.008	0.002	<0.008	0.003	<0.008	0.003	<0.008	0.003
$K^{D\times SA}[C_\alpha H_\alpha \cdot H_\alpha](\omega_H)$	0.011 ± 0.002	0.017[e]	0.017 ± 0.002	0.018[e]	0.0043 ± 0.0007	0.006[e]	0.021 ± 0.001	0.016[e]
$K^{D\times SA}[H_\alpha C_\alpha \cdot C_\alpha](\omega_C)$	-0.19 ± 0.02	−0.14[f]	-0.154 ± 0.009	−0.13[f]	-0.059 ± 0.007	−0.08[f]	-0.12 ± 0.01	−0.14[f]
		−0.08[g]		−0.08[g]		−0.05[g]		−0.08[g]
$K^{D\times SA}[H_\alpha C_\alpha \cdot C_\alpha](0)$	-0.37 ± 0.09	−0.65[f]	-0.26 ± 0.08	−0.50[f]	-2.2 ± 0.3	−2.6[f]	-0.25 ± 0.04	−0.46[f]
		−0.39[g]		−0.30[g]		−1.5[g]		−0.28[g]
$K^{D\times SA}[C'C_\alpha \cdot C_\alpha](\omega_C)$	≈0		≈0		≈0		≈0	
$K^{D\times SA}[C_\alpha C' \cdot C'](\omega_C)$	-0.038 ± 0.011	−0.044[h]	-0.047 ± 0.008	−0.039[h]	-0.018 ± 0.006	−0.017[h]	-0.042 ± 0.06	−0.055[h]
$J^{SA}[C'](\omega_C)$		0.16[h]		0.15[h]		0.075[h]		0.19[h]
ΔR_2[C−D]	-0.9 ± 0.2		-0.5 ± 0.2		-3.8 ± 0.8		-0.60 ± 0.12	
ΔR_2[E−F]	1.4 ± 0.4		1.0 ± 0.5		6.5 ± 1.8		0.9 ± 0.2	
ΔR_2[C−E]	-3.7 ± 0.5		-2.7 ± 0.4		-17.3 ± 1.6		-2.5 ± 0.3	
ΔR_2[D−F]	-1.7 ± 0.3		-1.3 ± 0.4		-7.1 ± 1.3		-1.10 ± 0.14	

[a] Calculated by ignoring $J^{SA}[C_\alpha]$. [b] Calculated assuming $\Delta\sigma[H_\alpha] = 5.2$ ppm. [c] Calculated assuming $\Delta\sigma'[C_\alpha] = -32$ ppm. [d] Calculated assuming $\Delta\sigma[C_\alpha] = 31.5$ ppm, $\eta = 1.0$. [e] Calculated assuming $\Delta\sigma[H_\alpha] = 4.4$ ppm. [f] Calculated assuming $\Delta\sigma'[C_\alpha] = -29$ ppm (calculated from $K^{D\times SA}[C_\alpha H_\alpha \cdot C_\alpha](\omega_C)$). [g] Calculated assuming $\Delta\sigma'[C_\alpha] = -17$ ppm (calculated from $K^{D\times SA}[C_\alpha H_\alpha \cdot C_\alpha](0)$). [h] Calculated assuming $\Delta\sigma[C'] = 120$ ppm, $\eta = 0.9$.

degree of anisotropic motion characterized by an internal diffusion constant, D_i ($1/\tau_i = 2D_i$), a well-known triexponential results:

$$J(\omega) \propto \mathrm{Re}\int_0^\infty \exp(-t/\tau_0)\{S_1^2 S_2^2 + (1 - S_2^2)\exp(-2t/\tau_i) + S_2^2(1 - S_1^2)\exp(-t/2\tau_i)\} \quad (5)$$

with $S_2^2 = (1/4)(4-3\sin^4\theta)$ and $S_1^2 = (3\cos^2\theta - 1)^2/(4-3\sin^4\theta)$. The angle θ is the polar angle between the axis of (internal) rotation and the principal axis of an axially symmetric rank two interaction (e.g., the dipole−dipole interaction).

In principle, the cross-correlated spectral density function could be described in a similar manner. For example, in the simplest case,[33]

$$K^{\eta\times\eta'}(\omega) \propto \mathrm{Re}\int_0^\infty \exp(-t/\tau_0)\{S_\eta S_{\eta'} + ({}^1/_2\,(3\cos^2\Theta_{\eta\eta'} - 1) - S_\eta S_{\eta'})\exp(-t/\tau_1)\}\exp(-i\omega t)\,dt \quad (6)$$

The angle $\Theta_{\eta\eta'}$ defines the angle between the axes (assuming axial symmetry) of the interfering (correlated) interactions, η and η'. More commonly, one utilizes a simpler, less general form:

$$K^{\eta\times\eta'}(\omega) \propto \mathrm{Re}\int_0^\infty {}^1/_2\,(3\cos^2\Theta_{\eta\eta'} - 1)\exp(-t/\tau_0)\{S^2 + (1 - S^2)\exp(-t/\tau_1)\}\exp(-i\omega t)\,dt \quad (7)$$

In practice, the general interpretation of relaxation data in context of either eq 6 or 7 is imprudent.

Regardless of what approach is used, before one can glean dynamical information from various NMR relaxation rates, an accurate set of interaction constants must be defined. Using standard cautions,[34] D-alanine dipole−dipole interaction strengths, ($\gamma_i\gamma_j\hbar\langle r_{ij}^{-3}\rangle$), are calculated as 13.8×10^4 s^{-1}, 1.87×10^4 s^{-1}, and 1.26×10^4 s^{-1}, for $C_\alpha H_\alpha$, $H_\alpha C'$ and $C'C_\alpha$ interactions, respectively. For glycine, the relevant values are 13.8×10^4 s^{-1} and 14.0×10^4 s^{-1} for the $C_\alpha H_\alpha$ and $H_\alpha H'_\alpha$ interactions. These values take into account that the C_α carbon deviates from standard tetrahedral geometry in both residues[21] for all of the conformers of deltorphin-I. For D-alanine, angles vary from 106.6° ($\angle C'C_\alpha H_\alpha$) up to 117.0° ($\angle C'C_\alpha C_\beta$) and for glycine, from 104.4° ($\angle H_\alpha C_\alpha H'_\alpha$) up to 116.6° ($\angle NC_\alpha C'$). As will be

(33) Elbayed, K.; Canet, D. *Mol. Phys.* **1989**, *68*, 1033−1046.

(34) Ottiger, M.; Bax, A. *J. Am. Chem. Soc.* **1999**, *121*, 4690−4695.

demonstrated later, if not taken into account, these deviations can induce significant errors in the calculated values of the cross-correlation spectral densities. Furthermore, the C_α angular values indicate that the $NC_\alpha C'$ plane of glycine bisects the $H_\alpha C_\alpha H'_\alpha$ angle whereas the $C'C_\alpha$ bond of D-alanine is not in the bisecting plane of the $H_\alpha C_\alpha C_\beta$ angle. Again, this will prove important in later discussion.

For the interpretation of the various spectral densities, both graphical and numerical analyses were used in context of a chosen model. In the graphical analysis, contour maps of one parameter versus another (for example, τ_0 versus τ_0/τ_i) were calculated from the experimental values of each dipole−dipole cross-correlation spectral density, cross-relaxation rate, and spin−lattice relaxation rate, $R_1[i]$, while the other dynamical parameters were locked to grid search values. For each map, the error associated with the experimental data yields two contours that define a range of possible values for these parameters. The overlap of all the ranges yields sets of dynamical parameters that are consistent with the dipolar data. Subsequently, the best set was determined by minimizing the target function,

$$\chi^2(\zeta) = (1/N)\,\Sigma_i[(V_i^{calc}(\zeta) - V_i^{exp})/\Delta V_i^{exp}]^2 \qquad (8)$$

where V_i^{calc} and V_i^{exp} are the calculated and experimental values, respectively. ΔV_i^{exp} is the standard deviation of the experimental value, index i runs over a set of spectral densities or appropriate combination of spectral densities, N is the number of experimental values considered, and ζ denotes the set of extracted motional parameters. We used this graphical method in previous work.[27] It is far more reliable than numerical minimization by computer as demonstrated by Jin et al.[35] Not only does such an analysis aid in visualizing which spectral densities are crucial and which are redundant, but also, it reveals how the errors in the data influence both the choice of the best set of parameters and their propagated error (the overlap region is never rectangular). Unfortunately, this graphical analysis is too cumbersome when more than five parameters must be determined.

The first model tested was that of slower isotropic overall tumbling with rapid, restricted, local motion.[8] Here, five parameters suffice to fit the dipolar data: one global correlation time τ_0 and two parameters per residue (one local correlation time τ_i and one order parameter S^2). As expected, the data do not support this simple description. For D-alanine, the required theoretical ratio of $(\sigma[C_\alpha H_\alpha])/(\sigma[C'H_\alpha]) = <r_{C_\alpha H_\alpha}{}^{-3}>^2/<r_{C'_\alpha H_\alpha}{}^{-3}>^2$ differs from the experimental ratio by a factor of 2, and for the glycine residue, no positive value of S^2 can reproduce the data.

Next, it was assumed that each residue behaved as an independent rigid symmetric top diffusional rotator. For this model, the theoretical expressions[36] require four parameters for D-alanine (diffusion constants, $D_\parallel$ and $D_\perp$, and the two angles needed to position the unique axis of the diffusion tensor with respect to the $C'C_\alpha H_\alpha$ plane) and three additional parameters are needed (one angle is required to position uniquely the motional axis with respect to the bisector of the $H_\alpha C_\alpha H_\alpha'$ angle) for glycine. The appropriate contour maps of τ_0 ($=1/6D_\perp$) versus $D_\parallel/D_\perp$ for the dipolar spectral densities reveal no internally consistent solution. Because this model fails for both residues, further discussion is unwarranted.

A model that considers anisotropic overall motion and anisotropic local motion implies a minimum of 10 fitting parameters. These include three molecular parameters (two overall correlation times and one mixing coefficient), four parameters for D-alanine (a local correlation time and three order parameters), and three parameters for glycine (a local correlation time and two order parameters). This model was abandoned because it is impossible to consider the simultaneous relationships of 10 parameters from a graphical analysis.

A sensible yet tractable model considers rotational jumps between two identical minima separated by an angle 2γ along with effective, isotropic local tumbling. The local isotopic correlation times are residue specific, that is, complex internal peptide motions dynamically decouple these residues. This model seemed particularly interesting since the calculations[21] made on deltorphin-I indicate that the φ_{D-Ala} angle equals $\approx 140° \pm 20°$ for the D-alanine residue in all the conformers whereas the ψ_{D-Ala} angle equals $\approx 80° \pm 15°$ and $\approx -150° \pm 15°$ for 60% of the conformers and 40% of the conformers, respectively. The reverse is obtained for glycine where ψ_{Gly} is nearly 180° for all conformers, but φ_{Gly} equals $\approx 80° \pm 15°$ and $\approx -80° \pm 15°$ for 60% of the conformers and 40% of the conformers, respectively.

In D-alanine, the molecular axis about which jumps occur is positioned by two angles (α and β) with respect to the $C'C_\alpha H_\alpha$ moiety. The angle β is the angle between the internal jump axis and the $C'C_\alpha$ bond axis whereas α is the dihedral angle between the plane defined by these two axes and the $C'C_\alpha H_\alpha$ plane. In glycine, one angle (β) positions the internal motional axis with respect to the bisector of the $H_\alpha C_\alpha H_\alpha'$ angle. Again, the motion of these two residues was considered as independent to take into account their different mobilities. Therefore, this model implies five parameters for D-alanine (τ_0, τ_i, γ, α, and β) with $1/\tau_i$ defined as twice the jump rate.[7] For glycine, the internal axis about which jumps occur is assumed to be collinear with the NC_α bond[16] thus reducing to three (τ_0, τ_i, γ) the number of parameters to be determined for this residue. The dipolar spectral densities associated with this model can be written in the form:[7]

$$J^D[ij](\omega) = (3/40)((\mu_o/4\pi)(\gamma_i\gamma_j\hbar<r_{ij}{}^{-3}>)^2\{(3\cos^2\theta_{ij} - 1)^2 J_0(\omega) + 12\cos^2\theta_{ij}\sin^2\theta_{ij}J_1(\omega) + 3\sin^4\theta_{ij}J_2(\omega)\} \quad (9)$$

$$K^{D\times D}[ij\cdot jk](\omega) = (3/40)((\mu_o/4\pi)(\gamma_j\hbar)^2\gamma_i\gamma_k<r_{ij}{}^{-3}><r_{ik}{}^{-3}>) \{(3\cos^2\theta_{ij} - 1)(3\cos^2\theta_{jk} - 1)J_0(\omega) + 12\cos\theta_{ij}\sin\theta_{ij}\cos\theta_{jk}\sin\theta_{jk}\cos(\phi_{ij} - \phi_{jk})J_1(\omega) + 3\sin^2\theta_{ij}\sin^2\theta_{jk}\cos(2\phi_{ij} - 2\phi_{jk})J_2(\omega)\} \quad (10)$$

where $J_m(\omega) = \cos^2(m\gamma)\tau_0/(1 + (\omega\tau_0)^2) + \sin^2(m\gamma)\tau_{0i}/(1 + (\omega\tau_{0i})^2)$ and $\tau_{0i} = \tau_0\tau_i/(\tau_0 + \tau_i)$. The polar angles, ($\theta_{jk}$, ϕ_{ij}), position the dipolar vectors relative to the internal jump axis and can be written in terms of α and β.

For glycine, the dynamics were determined from the following four dipolar rates: $R_1[C_\alpha] = 2\rho[C_\alpha H_\alpha]$, $\sigma[C_\alpha H_\alpha]$,

(35) Jin, D.; Figueiridо, F.; Montelione, G. T.; Levy, R. M. *J. Am. Chem. Soc.* **1997**, *119*, 6923−6924.
(36) Werbelow, L. G.; Grant, D. M. *Adv. Magn. Reson.* **1975,** *9*, 189−299.

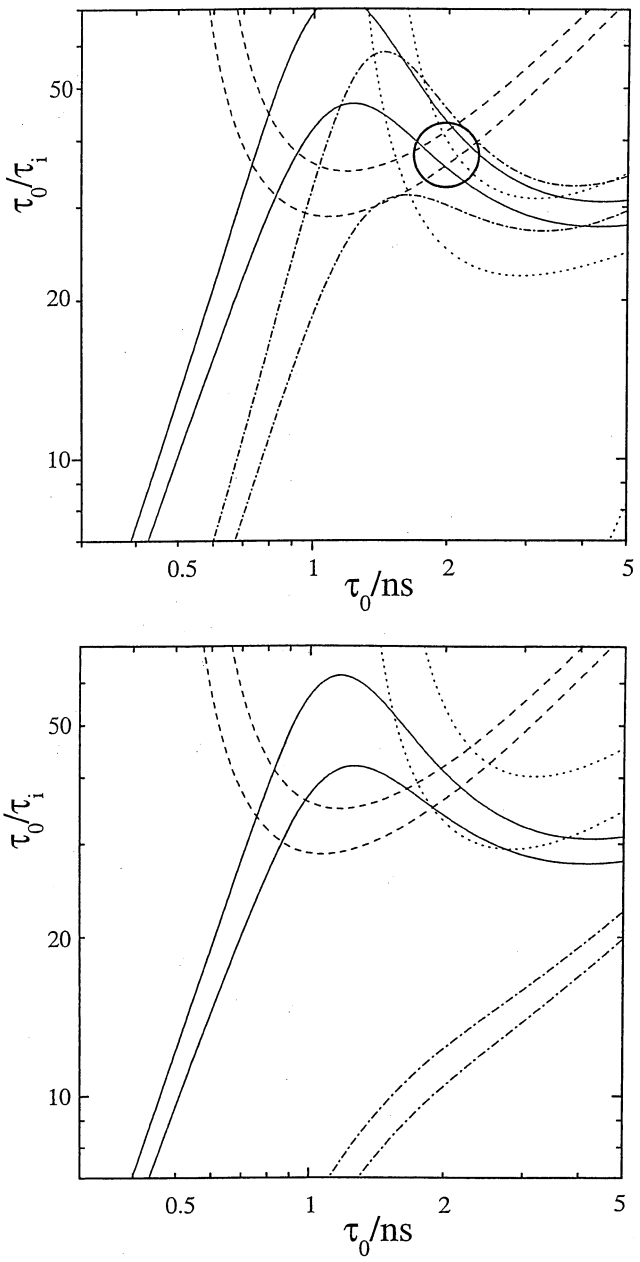

Figure 3. (a) Intersection (within the circled region) of the (τ_0/τ_i, τ_0) contour maps for different NMR relaxation parameters used to assess the dynamics of glycine in Solution II at 265 K: $R_1[C_\alpha]$, solid line; $\sigma[C_\alpha H_\alpha]$, dashed line (- - -); $K^{D\times D}[C'C_\alpha \cdot C_\alpha H_\alpha](\omega_C)$, dashed−dotted line (- · - ·); $K^{D\times D}$-$[C'H_\alpha \cdot H_\alpha C_\alpha](\omega_H)$, dotted line (· · · · ·). The contour lines correspond to the experimental values plus or minus one standard deviation. The jump angle, $\gamma = 68°$, and the dipolar interaction constants use the correct geometry. (b) Legend reads the same as for Figure 3a except dipolar interaction constants are evaluated using a standard, tetrahedral geometry.

$K^{D\times D}[C_\alpha H_\alpha \cdot H_\alpha H_\alpha'](\omega_H)$, and $K^{D\times D}[H_\alpha C_\alpha \cdot C_\alpha H_\alpha'](\omega_C)$ where $\rho[ij]$ is written as

$$\rho[ij] = \{(1/3)\, J^D[ij](\omega_i - \omega_j) + J^D[ij](\omega_i) + 2\, J^D[ij]\,(\omega_i + \omega_j)\} \quad (11)$$

The shielding anisotropy contribution to R_1 is negligible and is not considered at this point. Figure 3 demonstrates our procedure for determination of the dynamical parameters and illustrates the interplay of various terms. Figure 3a presents a contour map of these four dipolar relaxation rates plotted as a function of τ_0 and τ_0/τ_i for one particular γ value (68°). From this map, it is seen that consideration of auto-correlation terms alone (the solid and dashed lines) yields an ambiguous result as there are two pairs of parameters compatible with the data. Inclusion of cross-correlation terms is necessary to properly evaluate this system.

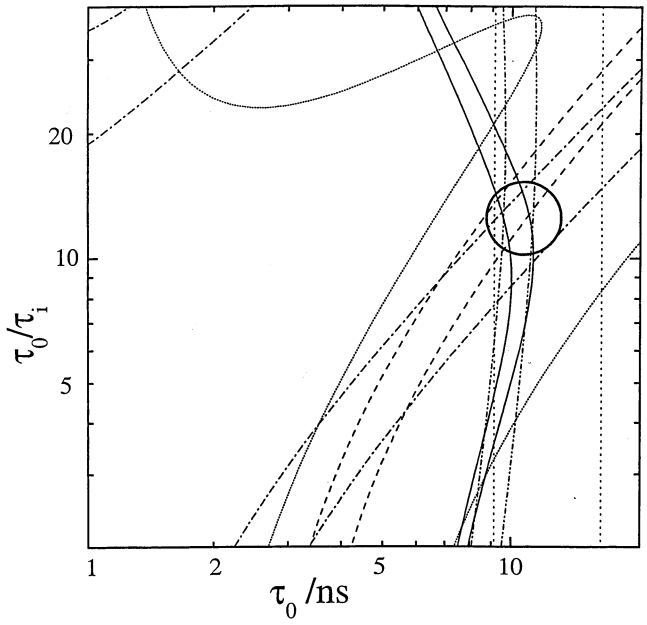

Figure 4. Intersection (within the circled region) of the (τ_0/τ_i, τ_0) contour maps for different NMR relaxation parameters used to assess the dynamics of D-alanine in Solution II at 265 K: $R_1[C_\alpha]$, solid line; $\sigma[C_\alpha H_\alpha]$, dashed line (- - -); $\sigma[H_\alpha C']$, dashed−dotted line(- · - ·); $\sigma[C'C_\alpha]$, dashed−dotted-dotted line (- ·· -); $K^{D\times D}[C'C_\alpha \cdot C_\alpha H_\alpha](\omega_C)$, dotted line (· · · · ·); $K^{D\times D}$-$[C'H_\alpha \cdot H_\alpha C_\alpha](\omega_H)$, short dotted line (··········). The jump angle, $\gamma = 74°$, and angles $\alpha = 40°$, $\beta = 22°$. The dipolar interaction constants use the correct geometry.

Also, the importance of considering deviations from tetrahedral geometry about C_α is revealed in Figure 3b. Although three of the relaxation terms are relatively insensitive to these angular considerations, $K^{D\times D}[H_\alpha C_\alpha \cdot C_\alpha H_\alpha'](\omega_C)$ is highly dependent on the effective $H_\alpha C_\alpha H_\alpha'$ angle. If recognized properly, this can be a tremendous asset for analysis. Conversely, if not properly recognized, the credibility of any dynamical description is severely compromised.[34]

For determination of the motion of D-alanine, the following rates were considered:

$R_1[C_\alpha] = \rho[C_\alpha H_\alpha] + \rho[C_\alpha C']$, $\sigma[C_\alpha H_\alpha]$, $\sigma[H_\alpha C']$, $\sigma[C'C_\alpha]$, $K^{D\times D}[C'C_\alpha \cdot C_\alpha H_\alpha](\omega_C)$, and $K^{D\times D}[C'H_\alpha \cdot H_\alpha C_\alpha](\omega_H)$. The same graphical approach described above was applied to these data. Understandably, this is more complicated because of the increased dimensionality of the parameter space. Figure 4 demonstrates one particular analysis for Solution II at 265 K (for the set of angles, $\alpha = 40°$, $\beta = 22°$, $\gamma = 74°$).

Although not obvious, it is relatively easy to explore this five-dimensional space, locate sets of parameters compatible with the experimental data, and then find the best set through application of eq 8. The result of this effort is summarized by the parameters listed in Table 2.

Discussion

Dynamics. The dynamic parameters presented in Table 2 are reasonable and internally consistent. For the glycine residue, the value of τ_0 at 298 K (0.65 ns) is similar to that found at 295 K (0.7 ns) using proton−proton NOEs assuming local,

Table 2. Summary of the Motional and Geometric Parameters that Best Fit the Dipolar Relaxation Rates

	Solution I		Solution II	
	298 K	310 K	265 K	314 K
		Glycine		
τ_0/ns	0.65 ± 0.07	0.47 ± 0.05	1.9 ± 0.2	0.53 ± 0.06
τ_0/τ_i	13 ± 1	11 ± 1	38 ± 3	13 ± 1
τ_i/ps	50 ± 6	42 ±8	50 ± 7	40 ± 6
γ	59° ± 1°	58° ± 1°	68° ± 1°	60° ± 1°
		D-Alanine		
τ_0/ns	4.1 ± 0.5	2.7 ± 0.3	10.0 ± 0.9	2.1 ± 0.4
τ_0/τ_i	6.4 ± 0.9	6.8 ± 1.0	12 ± 2	9 ± 2
τ_i/ns	0.65 ± 0.13	0.39 ± 0.08	0.81 ± 0.16	0.23 ± 0.08
α	120° ± 10°	110° ± 10°	40° ± 10°	65° ± 10°
β	30° ± 5°	30° ± 5°	22° ± 5°	18° ± 5°
γ	80° ± 4°	80° ± 4°	74° ± 1°	70° ± 2°

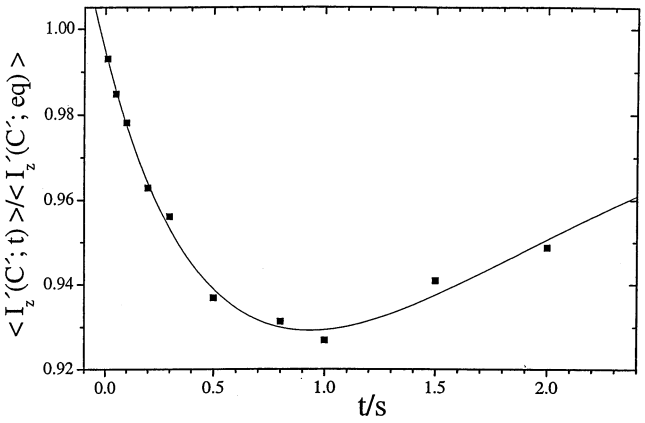

Figure 5. Plot of the normalized $^{13}C'$ magnetization of D-alanine versus the evolution time between perturbation (C_α inversion) and observation. This response is shown for Solution II at 265 K.

isotropic motion.[21] Likewise, the value of 2γ is close to the variation between conformers determined by calculation[21] ($\Delta\phi_{Gly} = 160° \pm 30°$). The similarity between the parameter values for solution I at 298 K and solution II at 314 K (temperatures where the two solutions have the same macroscopic viscosity) reveals that there is no notable solvent influence upon the local dynamics of this residue.

For D-alanine, the large value found for τ_0 at 265 K is quite unusual for an oligopeptide. However, it is clear from Figure 5 that the cross relaxation rate $\sigma[C'C_\alpha]$ is negative. This anomaly is easily explained by the possible auto-association of deltorphin-I at this low temperature and relatively high (20 mM) concentration. Also, the values of τ_0 are notably larger than those determined by proton−proton NOEs at ambient temperature (≈1 ns at 295 K) assuming local, isotropic motions.[21] This is in contrast to glycine where the internal correlation time, τ_i, has much less influence.[37]

For D-alanine, the noticeable difference in the angle α between solutions I and II reveals a significant yet subtle solvent influence on the local dynamics for this residue. Likewise, as Figure 6 illustrates, although the initial responses in a transient Overhauser experiment are similar, the overall response curves are markedly different. The value of $2\gamma \approx 160°$ lies close to the variation between conformers determined by calculation,[21]

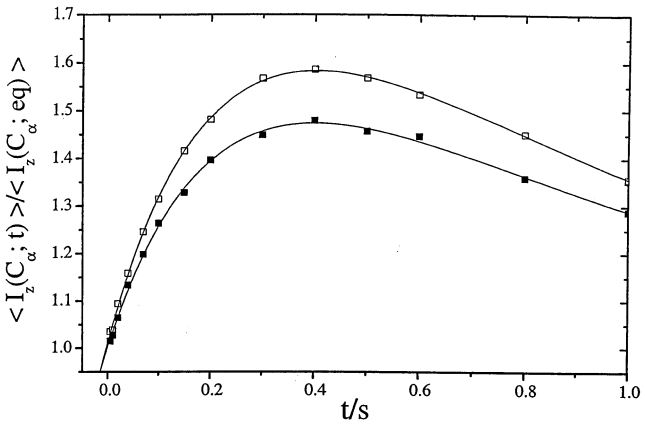

Figure 6. Plot of the normalized $^{13}C_\alpha$ magnetization of D-alanine versus the evolution time between perturbation (H_α inversion) and observation. This response is shown for Solution II at 314 K (open squares, upper curve) and for Solution I at 298 K (filled squares, lower curve).

$\Delta\psi_{D-Ala} = 130° \pm 30°$. The dynamics are relatively insensitive to changes in α (±10°) or β (±5°). However, the uniqueness of the fits are extremely sensitive to changes in γ (±1° at 265 K). This exquisite sensitivity obtains for both the glycine and D-alanine residues.

Using the parameters deduced by the described methodology and summarized in Table 2, the spectral densities themselves were recalculated. In Table 1, these calculated values are shown alongside the experimental values.

Shielding Anisotropies. Once a suitable dynamical model is chosen using well-defined interactions, it proves possible to examine confidently numerous other polarization/coherence transfer rates involving the nonaxially symmetric interactions. In principle, these interactions themselves could have been sed in our analysis to assess the dynamics but, in practice, this proves extremely difficult and fraught with assumption and ambiguity.

From the transfer rate, $S_z \Longrightarrow -4K^{D\times SA}[C_\alpha H_\alpha \cdot H_\alpha](\omega_H) \Longrightarrow 2I_zS_z$, one can explore properties of the H_α shielding tensor. If this tensor is axially symmetric ($\eta = 0$) and the principal component (σ_{zz}) aligns with the $C_\alpha H_\alpha$ axis, a value of $\Delta\sigma[H_\alpha] = 5.2 \pm 0.8$ ppm is deduced for the glycine residue. For the D-alanine residue, $\Delta\sigma[H_\alpha] = 4.4 \pm 1.6$ ppm. These are close to literature values.[38] The definition of the shielding anisotropy used in this work is $\Delta\sigma = \sigma_{zz} - (\sigma_{yy}+\sigma_{xx})/2$ with $\sigma_{zz} > \sigma_{yy} > \sigma_{xx}$. The shielding asymmetry,

$$\eta\ (0 \le \eta \le 3), \text{ is defined as } (3/2)(\sigma_{yy} - \sigma_{xx})/\Delta\sigma.$$

Assuming the orientation and symmetry of the proton shielding tensor simplified the evaluation of this parameter. Assessing the C_α and C' shielding tensors are more problematic and various approaches are possible.

First, we discuss the C_α carbon. A current approach considers only the projection of the C_α shielding tensor on the $C_\alpha H_\alpha$ axis.[39] Although rudimentary, this provides a simple, albeit somewhat ill-defined, estimate of an effective anisotropy, $\Delta\sigma'[C_\alpha] = \sigma_{||} - <\sigma_\perp>$ ($<\sigma_\perp>$ represents the average shielding perpendicular

(37) Zeng, L.; Fischer, M. W. F.; Zuiderweg., E. R. P. *J. Biomol. NMR* **1997**, *7*, 157−162.

(38) Sitkoff, D.; Case, D. A. *Prog. Nucl. Magn. Reson. Spectrosc.* **1998**, *32*, 165−90.

(39) Tjandra, N.; Bax, A. *J. Am. Chem. Soc.* **1997**, *119*, 9576−9577.

to the $C_\alpha H_\alpha$ axis) from the transfer rate,

$$I_z \Rightarrow -4K^{D\times SA}[C_\alpha H_\alpha \cdot C_\alpha](\omega_C) \Rightarrow 2I_zS_z \text{ or } I_+ \Rightarrow -(8/3)K^{D\times SA}[C_\alpha H_\alpha \cdot C_\alpha](0) - 2K^{D\times SA}[C_\alpha H_\alpha \cdot C_\alpha](\omega_C) \Rightarrow 2S_zI_+.$$

Three recent papers[40−42] discuss ramifications of this approach in more detail. Using the experimentally deduced values of $K^{D\times SA}[C_\alpha H_\alpha \cdot C_\alpha](\omega_C)$, an "effective" shielding anisotropy ($\Delta\sigma'[C_\alpha]$) of -32 ± 2 ppm is obtained for the glycine residue and -29 ± 7 ppm for the D-alanine residue. The expression given in ref 38 yields $\Delta\sigma'[C_\alpha] = -34$ ppm and -17 ppm for the glycine and D-alanine residues when taking into account the φ and ψ angles calculated for each of the conformers[21] of deltophin-I. Using the zero frequency spectral density, $K^{D\times SA}[C_\alpha H_\alpha \cdot C_\alpha](0)$, determined from differential line width variations, one obtains the value, $\Delta\sigma'[C_\alpha] = -17 \pm 4$ ppm for the D-alanine residue. However, when line width differential analysis is applied to the glycine multiplet, an unrealistically large value (about -50 ± 20 ppm) is found. We have no explanation for this presumed failure.

A much more satisfactory approach to this problem considers the complete shielding tensor. Relevant expressions[43] for $J^{SA}[i](\omega)$ and $K^{D\times SA}[ij\cdot j](\omega)$ are easily adapted to the present application yielding,

$$J^{SA}[i](\omega) = (1/30)(\Delta\sigma\gamma_i B_0)^2\{d_0J_0(\omega) + d_1J_1(\omega) + d_2J_2(\omega)\} \quad (12)$$

$$K^{D\times SA}[ij\cdot j](\omega) = (1/10)((\mu_o/4\pi)\hbar\gamma_i\gamma_j\langle r_{ij}^{-3}\rangle(\Delta\sigma\gamma_j B_0)\{d_{0'}J_0(\omega) + d_{1'}J_1(\omega) + d_{2'}J_2(\omega)\} \quad (13)$$

where $d_0 = 1/4(3\cos^2\beta^{SA} - 1)^2 - (\eta/2)(3\cos^2\beta^{SA} - 1)\sin^2\beta^{SA}\cos 2\alpha^{SA} + (\eta/2)^2\sin^4\beta^{SA}\cos^2 2\alpha^{SA}$, $d_1 = 3/4\sin^2 2\beta^{SA} + (\eta/2)\sin^2 2\beta^{SA}\cos 2\alpha^{SA} + (\eta^2/3)\sin^2\beta^{SA}(1 - \cos^2 2\alpha^{SA}\sin^2\beta^{SA})$, $d_2 = 3/4\sin^4\beta^{SA} - (\eta/2)\sin^2\beta^{SA}\cos 2\alpha^{SA}(\cos^2\beta^{SA} + 1) + (\eta^2/3)(1 - \sin^2\beta^{SA} + 1/4\cos^2 2\alpha^{SA}\sin^4\beta^{SA})$, $d_{0'} = 1/4(3\cos^2\beta^D - 1)(3\cos^2\beta^{SA} - 1 - \eta\sin^2\beta^{SA}\cos 2\alpha^{SA})$, $d_{1'} = (3/2)\sin 2\beta^D\sin\beta^{SA}\{\cos\beta^{SA}\cos(\gamma^D - \gamma^{SA}) + (\eta/3)[\cos 2\alpha^{SA}\cos\beta^{SA}\cos(\gamma^D - \gamma^{SA}) + \sin 2\alpha^{SA}\sin(\gamma^D - \gamma^{SA})]\}$,

$d_{2'} = 3/4\sin^2\beta^D\{\sin^2\beta^{SA}\cos(2\gamma^D - 2\gamma^{SA}) - (\eta/3)[\cos 2\alpha^{SA}(\cos^2\beta^{SA} + 1)\cos(2\gamma^D - 2\gamma^{SA}) + 2\sin 2\alpha^{SA}\cos\beta^{SA}\sin(2\gamma^D - 2\gamma^{SA})]\}$, and the $J_m(\omega)$ were introduced earlier in eqs 9 and 10. These coefficients, d and d', require introduction of the Euler angles ($\alpha^D = 0$, β^D, γ^D) and (α^{SA}, β^{SA}, γ^{SA}) which orient these two interfering interactions relative to the motional (jump) axis. (These Euler angles should not be confused with the angles α and β introduced earlier.)

In the present study, this approach is only practical for glycine. Here, the local site symmetry can be assumed as C_{2v} implying that σ_{yy} and σ_{zz} lie in the $C'C_\alpha N$ plane.[44,45] Hence, $\alpha^{SA} = \gamma^{SA} = 90°$. For the $C_\alpha H_\alpha$ axis, $\beta^D = 109.0°$ and $\gamma^D = -33.3°$. Thus, only three parameters must be deduced, $\Delta\sigma$, η, and β^{SA} where β^{SA} is the angle between σ_{zz} and the NC_α axis. We now calculate $\chi^2 = (1/4)\Sigma[(V^{calc} - V^{exp})/\Delta V^{exp}]^2$ where $V = K^{D\times SA}[C_\alpha H_\alpha \cdot C_\alpha](\omega_C)$ and the summation extends over thefour experimentally deduced values of $K^{D\times SA}[C_\alpha H_\alpha \cdot C_\alpha](\omega_C)$. In Figure 7, a contour plot of χ^2 is displayed as a function of η and β^{SA} for a $\Delta\sigma = 30$ ppm. These curves clearly demonstrate that for a given $\Delta\sigma$, χ^2 is minimized by an entire family of η and β^{SA} values (e.g., $\eta = 2.5$, $\beta^{SA} = -75°$ or $55°$; $\eta = 2.0$, $\beta^{SA} = -40°$ or $20°$, $\eta = 1.5$, $\beta^{SA} = -20°$ or $0°$; etc.). Similar curves were generated for a range of $\Delta\sigma$ values and in Figure 8, the variation of η versus β^{SA} at the χ^2 minimum is plotted for three different $\Delta\sigma$ values. It is important to recognize that in this relatively well-defined example, relaxation fails to discriminate between possible values of our three parameters and all of the sets implicit in Figure 8 are equally "good." However, if one

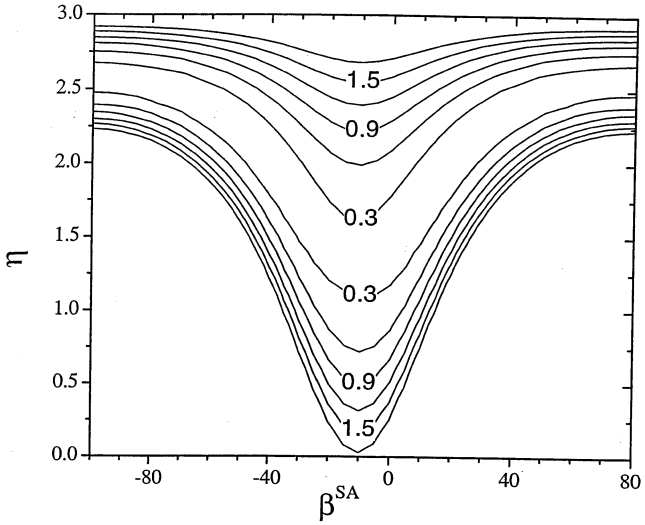

Figure 7. Contour plot of χ^2 as a function of asymmetry (η) and orientation (β^{SA}) for the C_α shielding tensor of glycine. A shielding anisotropy ($\Delta\sigma$) of 30 ppm is assumed.

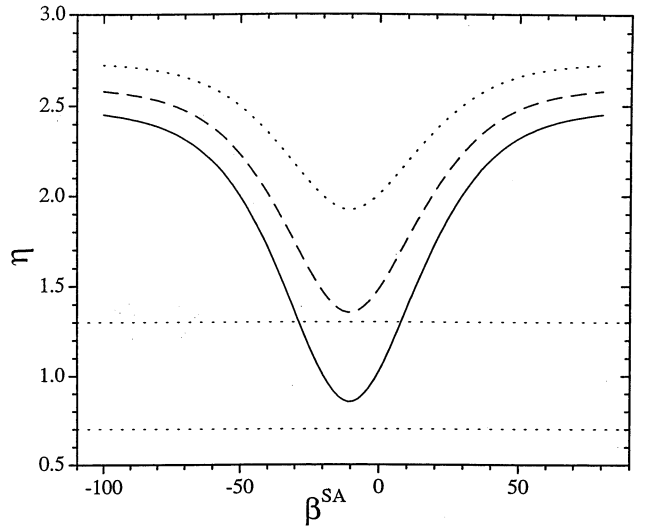

Figure 8. Continuation of Figure 7 showing variation of η versus β^{SA} at the χ^2 minimum for different values of $\Delta\sigma$ (28 ppm uppermost dotted line, 30 ppm dashed line, 32 ppm lower solid line).

(40) Hong, M. *J. Am. Chem. Soc.* **2000**, *122*, 3762−70.
(41) Havlin, R. H.; Lewis, D. D.; Bitter, H.-M. L.; Sanders, L. K.; Sun, H.; Grimley, J. S.; Wemmer, D. E.; Pines, A.; Oldfield, E. *J. Am. Chem. Soc.* **2001**, *123*, 10362−10369.
(42) Sun, H.; Sanders, L. K.; Oldfield, E. *J. Am. Chem. Soc.* **2002**, *124*, 5486−5495.
(43) Chung, J.; Oldfield, E.; Thevand, A.; Werbelow, L. G. *J. Magn. Reson.* **1992**, *100*, 69−81.
(44) Haberkorn, R. A.; Stark, R. E.; van Willigen, H.; Griffen, R. G. *J. Am. Chem. Soc.* **1981**, *103*, 2534−2539.
(45) Ando, S.; Ando, I.; Shoji, A.; Ozaki, T. *J. Mol. Struct.* **1989**, *192*, 153−161.

Table 3. Summary of the Orientational Parameters That Position the C′ Shielding Tensor and the C′C_α Dipolar Axis in D-Alanine Relative to the Twofold Jump Axis[a]

	solution I		solution II	
Euler angle	298 K	310 K	265 K	314 K
$\alpha^{SA}[C']$	188°	183°	178°	182°
$\beta^{SA}[C']$	118°	116°	86°	95°
$\gamma^{SA}[C']$	71°	61°	10°	15°
$\beta^{D}[C'C\alpha]$	30°	30°	22°	18°
$\gamma^{D}[C'C\alpha])$	90°	90°	90°	90°

[a] The uncertainty in these angular values is ±5° except for $\gamma^{SA}[C']$ (±10°) and for $\gamma^{D}[C'C_\alpha]$, which is defined.

uses the literature value[46] for η (1.0 ± 0.3), the derived $\Delta\sigma$ value for glycine is 32 ± 2 ppm with the principal component near the $C_\alpha N$ axis. (The opposite signs for $\Delta\sigma$ and $\Delta\sigma'$ result from different conventions and the choice of different principal axes. Indeed, other choices exist!)

This $\Delta\sigma$ value is at the upper limit of values in the literature.[46] Using $\Delta\sigma = 32$ ppm, $\eta = 1.0$, and $\beta^{SA} = -10°$, the spectral densities $J^{SA}[C_\alpha](\omega_C)$ and $K^{D\times SA}[C_\alpha H_\alpha \cdot C_\alpha](\omega_C)$ are calculated and reported in Table 1. As expected, $J^{SA}[C_\alpha](\omega_C)$ is very small and our neglect of this term in our previous analysis involving $R_1[C_\alpha]$ was justified.

The lack of any local symmetry for C_α in D-alanine coupled with the large range of literature[41,46] values for $\Delta\sigma$ and η makes it impossible to evaluate these parameters for this carbon given our rather limited set of experimental data.

The shielding tensor of C′ in alanine has been extensively studied and is well characterized ($\Delta\sigma = 120$ ppm, $\eta = 0.9$).[46] Because the component σ_{zz} is perpendicular to the peptide plane, there are only two undefined parameters, β', the angle between σ_{xx} and the $C'N_{Phe}$ axis, and ψ_{D-Ala}, which must be considered for defining the angles, (α^{SA}, β^{SA}, γ^{SA}). Using elementary trigonometic relationships, it is a simple matter to define α^{SA}, β^{SA}, γ^{SA} in terms of the angles α and β, determined from the dynamics, and β' and ψ_{D-Ala}. Using eqs 12 and 13, $J^{SA}[C'](\omega_C)$ and $K^{D\times SA}[C_\alpha C'\cdot C'](\omega_C)$ were calculated. Values of β' and ψ_{D-Ala} were obtained by minimizing the sum of $[(V_i^{cal} - V_i^{exp})/V_i^{exp}]^2$ where V_i are the two spectral densities, $J^{SA}[C'](\omega_C)$ and $K^{D\times SA}[C_\alpha C'\cdot C'](\omega_C)$. The experimental value for $J^{SA}[C'](\omega_C)$ was assumed to equal $(1/4)\{R_1[C'] - \rho[C'H_\alpha] - \rho[C_\alpha C']\}$. The minimization yields $\beta' = 41°$ and $\psi_{D-Ala} = 190°$. The relevant Euler angles are summarized in Table 3 and the calculated $J^{SA}[C'](\omega_C)$ and $K^{D\times SA}[C_\alpha C'\cdot C'](\omega_C)$ are reported in Table 1 alongside the corresponding experimental values.

The β' value is in excellent agreement with the value determined for the L-alanine residue.[46] Apparently, the chirality of the residue has no significant effect on the orientation of the C′ shielding tensor (as noted previously in the literature[47]). The value for ψ_{D-Ala} is intermediate between the values 80° ± 15° and 210° ± 15° calculated[21] for the main families of conformers.

Conclusion

In this study, it has proven possible to determine, accurately, a large number of cross-correlated spectral densities. The associated correlation coefficients provide a discriminatory set of model independent parameters that must be rationalized. As in previous studies,[27,48] a set of well-defined dipole−dipole interactions are utilized to clarify the molecular dynamics. In the present study, the simplest model capable of satisfactorily fitting the data was one of slower, site-specific, isotropic motion with a faster, anisotropic, two-site jump. More importantly, this model is consistent with the behavior expected from previous theoretical work.[21]

There are some simple lessons to be learned from the presented work. In the absence of constraints imposed by a cross-correlation, a provably incorrect dynamical model would have been obtained. Likewise, if simple, approximate molecular structures are assumed, dramatically different (presumably incorrect) dynamical interpretations would result. The extreme sensitivity of certain polarization transfer rates to assumed molecular geometry in conjunction with motional anisotropies cannot be overemphasized. For the D-alanine residue, a curious influence of solvent upon the dynamics was seen—an effect unrelated to the macroscopic viscosity.

Finally, once an internally consistent picture of the dynamics was generated, it was possible to refocus on finer features associated with the nuclear spin relaxation experiment.[27,48] In the present investigation, the anisotropy, asymmetry, and orientation of various shielding tensors were determined. The deduced parameters are in excellent agreement with literature values. No notable difference was seen for the shielding tensor of C′ for the D isomer of alanine when compared with the oft studied L-isomer.

Although the experimental requirements can be demanding and certain care must be exercised, the use of relaxation-induced polarization transfer—utilized in one form or another—will continue to grow in importance as the biochemical community becomes more familiar with the potential of the methodology.

Acknowledgment. We thank Dr. N. Leygue (LADIR) for sample synthesis, Mr. J. P. Forgerit (LADIR) for programming the graphical analysis, and Professor D. M. Grant (Utah) for use of instrument facilities. We are indebted to Professor Jozef Kowalewski for stimulating discussions. Support from the Swedish Foundation for International Cooperation in Research and Higher Education is acknowledged.

JA020772Q

(46) Wei; Y.; Lee, D.-K.; Ramamoorthy, A. *J. Am. Chem. Soc.* **2001**, *123*, 6118−6126.
(47) Ye, C. H.; Fu, R. Q.; Hu, J. Z.; Hou, L.; Ding, S. W. *Magn. Reson. Chem.* **1993**, *31*, 699−704.
(48) Coupry, C.; Chenon, M.-T.; Werbelow, L. G. *J. Phys. Chem.* **1994**, *101*, 899−904. Chenon, M.-T.; Coupry, C.; Werbelow, L. G. *J. Phys. Chem.* **1992**, *96*, 561−566.